IEEE Access
Multidisciplinary | Rapid Review | Open Access Journal

Received November 18, 2019, accepted December 6, 2019, date of publication December 17, 2019,
date of current version December 27, 2019.

Digital Object Identifier 10.1109/ACCESS.2019.2960438

A Snapback-Free and Low-Loss RC-IGBT With Lateral FWD Integrated in the Terminal Region

WEIZHONG CHEN[1,2], YAO HUANG[1], SHUN LI[1], YI HUANG[1], AND ZHENGSHENG HAN[2,3]

[1]College of Electronics Engineering, Chongqing University of Posts and Telecommunications, Chongqing 400065, China
[2]Institute of Microelectronics of Chinese Academy of Sciences, Beijing 100029, China
[3]Department of Microelectronics, University of Chinese Academy of Sciences, Beijing 100049, China

Corresponding author: Yao Huang (463087242@qq.com)

This work was supported in part by the National Nature Science Foundation of China under Grant 61604027 and Grant 61704016, and in part by the Chongqing Technology Innovation and Application Development (Key Industry Research and Development) under Grant cstc2018jszx-cyzd0646.

ABSTRACT A novel Reverse Conduction Insulated Gate Bipolar Transistor (RC-IGBT) with Lateral Free-Wheeling Diode (FWD) integrated in the Termination is proposed and investigated by simulation, named LDT-RC-IGBT. Firstly, the Equi-Potential Ring (EPR) of the termination acts as an anode and the N-Stopper/N-Collector of the termination acts as the cathode of the anti-parallel built-in diode. The N-Stopper/N-Collector is shorted to the P-Collector, and it also acts as the electric filed stopper in the breakdown state. Secondly, the N-Collector and the P-Collector are designed apart at the surface and bottom, respectively. Thus the short effect of the N-Collector of the conventional RC-IGBT is avoided, and the snapback is completely eliminated. Thirdly, the P-Collector is not replaced by the N-Collector so that the hole injection is much higher than the conventional RC-IGBT, thus the forward voltage drop (V_{on}) can be reduced remarkably, which is favorable to the decrease of conducting energy loss. The results show that, the LDT-RC-IGBT not only eliminates the snapback but also reduces V_{on}, it achieves a better trade-off between V_{on} and turn-off loss E_{off}. At the same V_{on} of 1.27 V, the E_{off} of LDT-RC-IGBT is 2.06 mJ/cm^2, which is 35.2%, 45.2% and 46.3% lower than that of the conventional RC-IGBT(3.19 mJ/cm^2), TPRC-IGBT(3.78 mJ/cm^2) and DARC-IGBT(3.85 mJ/cm^2), respectively. At the same E_{off} of 3.10 mJ/cm^2, the V_{on} of LDT-RC-IGBT is 1.17 V, which is 10% and 15.8% lower than that of the conventional RC-IGBT(1.30 V) and the DARC-IGBT(1.39 V), respectively.

INDEX TERMS RC-IGBT, breakdown voltage, turn-off, snapback.

I. INTRODUCTION

The Reverse Conducting Insulated Gate Bipolar Transistor (RC-IGBT) is a promising device by incorporating the IGBT and the FWD in a monolithic chip, which is widely used in the power converters [1]–[3]. For the conventional RC-IGBT, the FWD is vertically integrated in the active cell region by taking the place of partial P-Collector with N-Collector in the backside of the IGBT [4], [5]. However, several drawbacks especially an undesirable snapback phenomenon and high forward voltage drop (V_{on}) are induced by the short effect of the N-Collector at the forward conduction, which can prevent the device full turn-on and induces large conducting energy loss, respectively [6], [7]. Many advanced and complicated structures have been proposed to solve these issues in recent years [8]–[12], the TPRC-IGBT can suppress the snapback by the introduction of the Trench Oxide Layer (TOL) and P-float layer in the collector [13], but it is very complicated and hard to fabricate. The DARC-IGBT can not only suppress the snapback but also decrease the V_{on} by introducing the double anode [14]. However, it is at the cost of the Breakdown Voltage (BV) and turn-off losses (E_{off}), and it is also complicated. The Bi-mode Insulating Gate Transistor (BIGT) was developed to increase the $R_{n-buffer}$ by enlarging the collector size, but the current distribution and the turn-off performances can be further improved [15]. The CTG-RC-IGBT can eliminate the snapback completely, but the extra gate and signal are needed [16]. Moreover,

The associate editor coordinating the review of this manuscript and approving it for publication was Gian Domenico Licciardo.

TABLE 1. The key parameters for the devices.

Parameter	Con	DARC	TPRC	Proposed
Width	335μm	335μm	335μm	335μm
Ti	60μm	60μm	60μm	60μm
Ndrift	$1\times10^{14}cm^{-3}$	$1\times10^{14}cm^{-3}$	$1\times10^{14}cm^{-3}$	$1\times10^{14}cm^{-3}$
$N_{N\text{-}collector}$	$1\times10^{19}cm^{-3}$	$1\times10^{19}cm^{-3}$	$1\times10^{19}cm^{-3}$	$1\times10^{19}cm^{-3}$
$L_{N\text{-}collector}$	5μm	3μm	22μm	17μm
$J_{Nco\ or}\ L_{Nco}$	2μm	2μm	2μm	13μm
$N_{P\text{-}collector}$	$4\times10^{17}cm^{-3}$	$4\times10^{17}cm^{-3}$	$4\times10^{17}cm^{-3}$	$4\times10^{17}cm^{-3}$
$L_{P\text{-}collector}$	330μm	332μm	312μm	335μm
$N^{+}_{emitter}$	$1\times10^{20}cm^{-3}$	$1\times10^{20}cm^{-3}$	$1\times10^{20}cm^{-3}$	$1\times10^{20}cm^{-3}$
N_{buffer}	$1\times10^{16}cm^{-3}$	$1\times10^{16}cm^{-3}$	$1\times10^{16}cm^{-3}$	$1\times10^{16}cm^{-3}$
$L_{P\text{-}float}$	---	---	12μm	---
$N_{P\text{-}float}$	---	---	$3\times10^{16}cm^{-3}$	---
L_{SiO2}	---	---	1μm	---
T_{SiO2}	---	---	6μm	---
$L_{P\text{-}collector2}$	---	11μm	---	---
$T_{P\text{-}collector2}$	---	2μm	---	---
$N_{P\text{-}collector2}$	---	$6\times10^{16}cm^{-3}$	---	---

the FWDs of the above structures are vertically integrated in the active cell region, and the P-body acts as the anode and the N-Collector acts as the cathode.

In this paper, a novel RC-IGBT with Lateral FWD in the terminal region (LDT-RC-IGBT) is proposed and investigated to eliminate the snapback, and achieve better trade-off between V_{on} and E_{off}. This paper is implemented by the TCAD MEDICI, the mobility models including the CONMOB, PRPMOB, and FLDMOB are selected. The recombination and generation models including the Auger, Shockley–Read–Hall, and IMPACT.I are adopted, and the bandgap narrowing modeling BGN is also selected.

II. DEVICE STRUCTURE AND KEY PARAMETERS

The key parameters of the proposed LDT-RC-IGBT, conventional RC-IGBT, DARC-IGBT with additional anode and TPRC-IGBT with TOL and P-float are compared and listed in the Table. 1.

Fig. 1 shows the cross section schematic and corresponding equivalent circuit of the proposed LDT-RC-IGBT. It is divided into the active cell region with Metal-Oxide-Semiconductor (MOS) structure and the terminal region with Equi-Potential Ring (EPR), Field Limiting Ring (FLR) and N-stopper. It is note that the N-stopper is also acts as the N-Collector, which is designed at the surface of the chip and it is separated from the P-Collector in the bottom. The EPR and N-Stopper/N-Collector are shorted to the Emitter and P-Collector, respectively. Furthermore, the EPR acts as the anode and the N-Stopper/N-Collector acts as the cathode of the FWD, thus the FWD is laterally integrated in the terminal region and anti-parallel with the IGBT from the equivalent circuit.

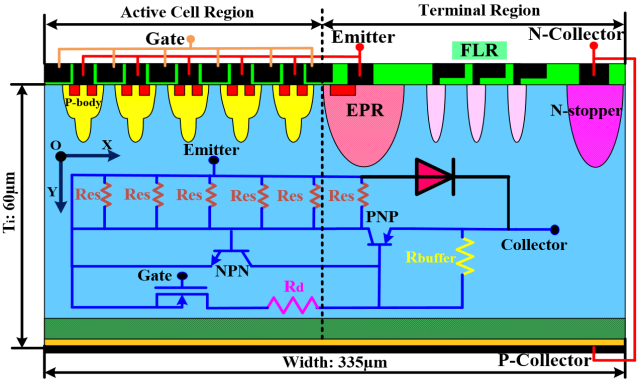

FIGURE 1. The cross section schematic of the proposed LDT-RC-IGBT. The FWD is laterally integrated by the EPR and N-stopper in the termination, and it is anti-parallel with the IGBT between the Emitter and the Collector from the equivalent circuit.

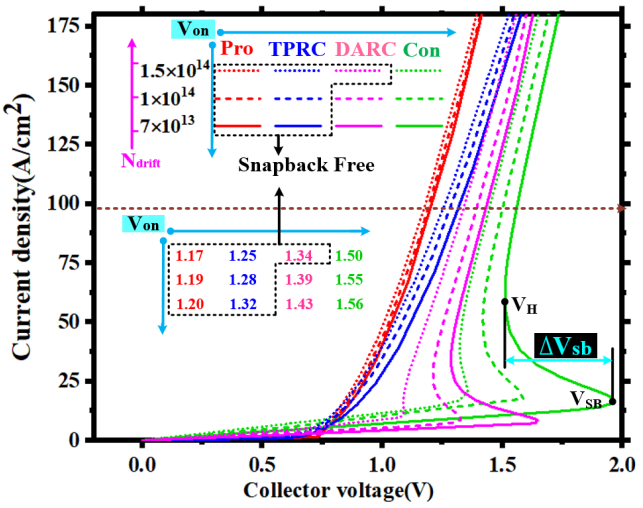

FIGURE 2. Forward conduction characteristics of the conventional RC-IGBT, the DARC-IGBT with additional anode, the TPRC-IGBT with Trench oxide and P-float, and the proposed with separated N-Collector and P-Collector. The V_{on} is extracted at the current density of 100 A/cm^2 and the snapback is $\Delta V_{sb} = V_{SB} - V_H$.

III. RESULTS AND DISCUSSION

A. FORWARD CONDUCTION CHARACTERISTICS

Fig. 2 illustrates the forward conduction characteristics for the conventional RC-IGBT (in [17]), TPRC-IGBT (in [13]), DARC-IGBT (in [14]) and the proposed LDT-RC-IGBT. For the conventional RC-IGBT, the FWD is integrated by replacing partial P-Collector with N-Collector in the bottom of the chip, as a result, an obvious snapback is observed due to the short effect of the N-Collector, and the device will change from unipolar to bipolar mode with abrupt current. Additionally, the forward voltage drop V_{on} is increased due to the decrease of the hole injection from the P-Collector. For the DARC-IGBT, the short effect of the N-Collector can be shielded by the additional anode and the snapback is suppressed to some extent. For the TPRC-IGBT, the N-Collector is shielded by the P-float and the uniploar mode

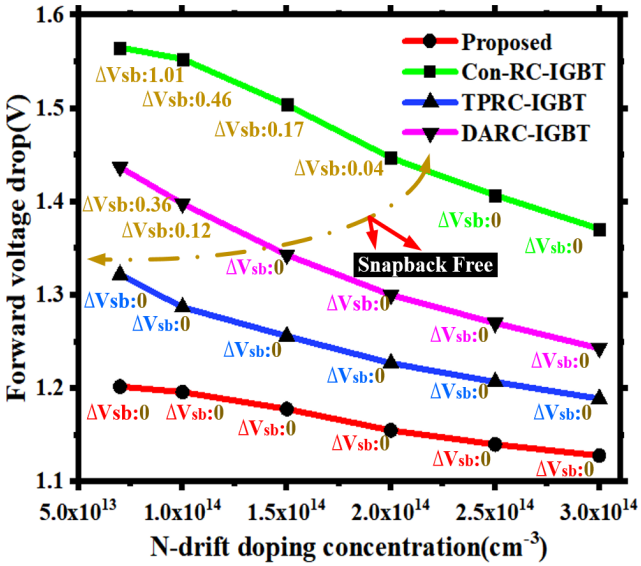

FIGURE 3. Dependence of the V_{on} and ΔV_{sb} (as shown in Fig. 2) on N_{drift} for the proposed LDT-RC-IGBT, conventional RC-IGBT, TPRC-IGBT and the DARC-IGBT.

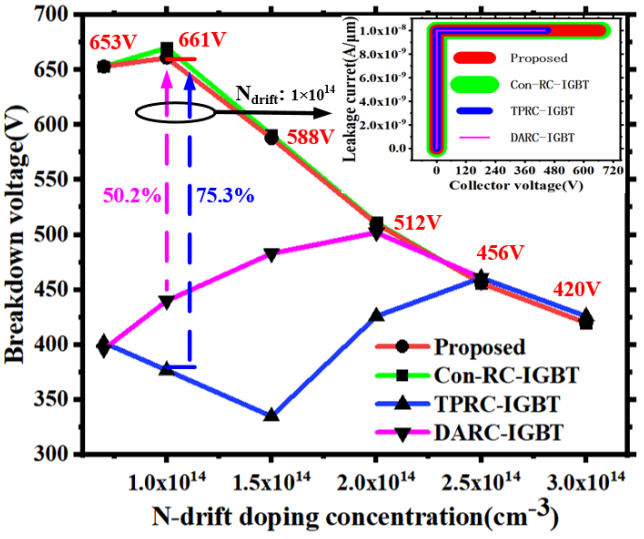

FIGURE 4. Dependence of the *BV* performance on N_{drift} for the proposed LDT-RC-IGBT, conventional RC-IGBT, TPRC-IGBT and DARC-IGBT. The inset picture shows the corresponding breakdown *I-V* curves for the devices at the N_{drift} of 1×10^{14}cm^{-3}.

is obstructed by the Trench oxide, thus the snapback is eliminated. However, the P-Collector is also partial replaced by the N-Collector, and the V_{on} is increased.

For the proposed, the N-Collector is designed with N-stopper at the surface of the chip, which is separated from the P-Collector at the bottom, thus the short effect is avoided and the snapback is completely eliminated. Moreover, the hole injection of the P-Collector is much higher than the other RC-IGBTs and the conduction loss is much lower. As a result, the V_{on} of the proposed is decreased from 1.20 V to 1.17 V at the current of 100A/cm^2, when the N-drift doping (N_{drift}) is increased from 7×10^{13} cm^{-3} to 1.5×10^{14} cm^{-3}, which is much lower than the other RC-IGBTs.

Fig. 3 shows the influence of the N_{drift} on the V_{on} and the snapback ΔV_{sb} for the RC-IGBTs. The V_{on} is decreased obviously with the increases of the N_{drift} for all the RC-IGBTs. Note that the V_{on} of the proposed is much lower than the others when the N_{drift} changes from 7×10^{13} cm^{-3} to 1.5×10^{14} cm^{-3}. Additionally, the ΔV_{sb} of the proposed and the TPRC-IGBT can be completely eliminated while the conventional RC-IGBT and DARC-IGBT can be partial suppressed.

B. REVERSE BREAKDOWN CHARACTERISTICS

Fig. 4 shows the dependence of *BV* on the N_{drift} at the breakdown state, and Fig. 5 illustrates the corresponding surface electric field ($E_{surface}$) at $Y = 6$ μm and the bulk electric field (E_{bulk}) at $Y = 15$ μm for the RC-IGBTs, respectively. It shows that the BV of the proposed is almost the same as the conventional RC-IGBT when the N_{drift} increases from 7×10^{13} cm^{-3} to 1.5×10^{14} cm^{-3}, due to the $E_{surface}$ and E_{bulk} of the active cell region and the terminal region are almost the same for the two devices. Additionally, the $E_{surface}$ and E_{bulk} of the TPRC-IGBT and DARC-IGBT are much lower at the

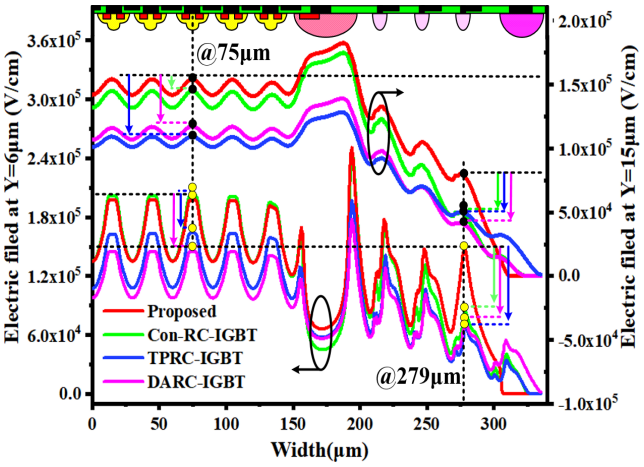

FIGURE 5. The surface electric field distributions $E_{surface}$ at Y=6 μm and the bulk electric field distributions E_{bulk} at Y=15 μm for the both active cell region and terminal region of the RC-IGBTs.

active cell region. The breakdown current-voltage curves are given in the inset picture of Fig. 4, the breakdown leakage current are set as 1×10^{-8}A/μm for all the devices, it shows that the proposed and the conventional RC-IGBT can obtain higher *BV* than the TPRC-IGBT and DARC-IGBT. As a result, the proposed LDT-RC-IGBT achieves a maximum *BV* of 661V at the N_{drift} of 1×10^{14}cm^{-3}, and it is increased by 50.2% and 75.3% compared to the DARC-IGBT with 440 V and TPRC-IGBT with 377 V, respectively.

Fig. 6 shows the trade-off relationships between V_{on} and *BV* of the RC-IGBTs when the N_{drift} increases from 7×10^{13} cm^{-3} to 3×10^{14} cm^{-3}. It shows that the V_{on} increases gradually from 1.12 V to 1.19 V for the proposed while it increases rapidly from 1.37 V to 1.54 V for the conventional RC-IGBT with the *BV* variation from 420 V to 661 V. For the

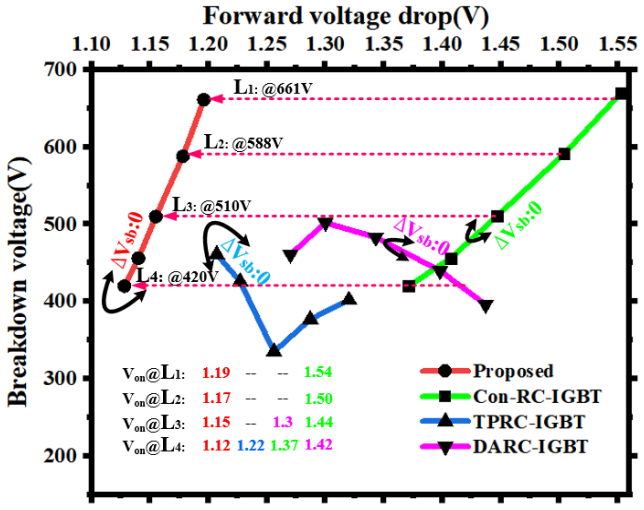

FIGURE 6. The trade-off between V_{on} and BV of the proposed LDT-RC-IGBT, conventional RC-IGBT, TPRC-IGBT and the DARC-IGBT with the N_{drift} variation from 7×10^{13} cm^{-3} to 3×10^{14} cm^{-3}.

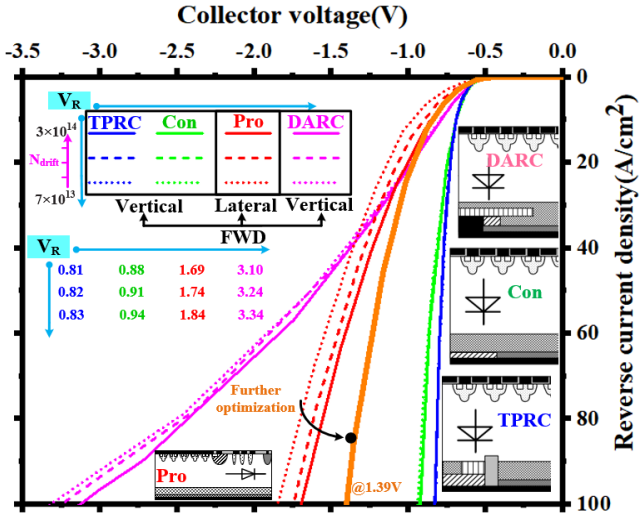

FIGURE 7. The reverse conduction characteristics of the FWDs for the proposed LDT-RC-IGBT, conventional RC-IGBT, TPRC-IGBT and the DARC-IGBT. The V_R is extracted at the current density of 100 A/cm^2.

TPRC-IGBT and the DRC-IGBT, it can be seen that the V_{on} are much higher than the proposed at the BV of 420 V, thus the proposed LDT-RC-IGBT achieves a better trade-off property without ΔV_{sb}.

C. REVERSE CONDUCTION CHARACTERISTICS

Fig. 7 gives the reverse conduction property of FWDs for the RC-IGBTs. The FWDs are vertically integrated in the active cell region by the P-body and the N-Collector for the conventional RC-IGBT, TPRC-IGBT and the DARC-IGBT. However, the FWD is laterally integrated in the terminal region by the EPR and the N-stopper/N-Collector for the proposed as shown in the inset picture. The reverse voltage drop V_R of the FWDs are compared with the N_{drift} variation from 7×10^{13} cm^{-3} to 3×10^{14} cm^{-3}. The conventional

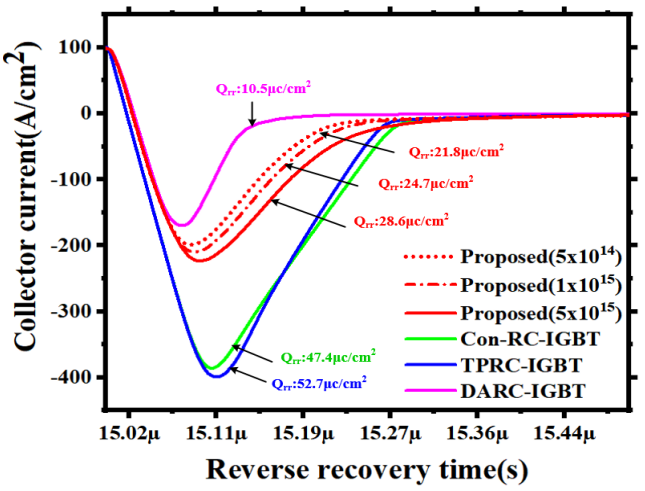

FIGURE 8. The reverse recovery waveforms of the RC-IGBTs. V_{bus} = 350 V, J_f = 100 A/cm^2, stray inductance Ls = 6 μH. The doping of the EPR for the proposed is decreased from 5×10^{15} cm^{-3} to 5×10^{14} cm^{-3}.

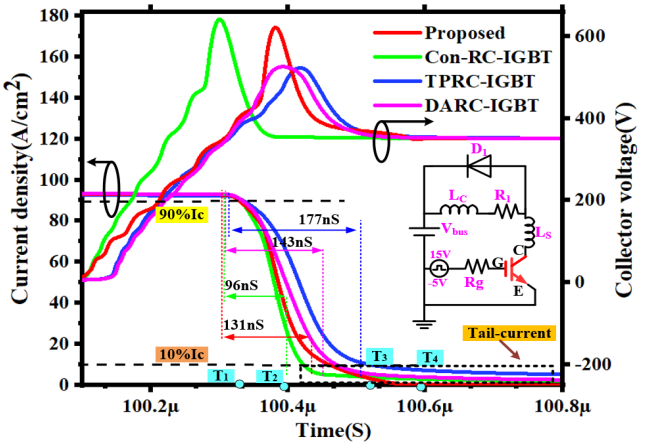

FIGURE 9. The turn-off current-time and voltage-time for the proposed LDT-RC-IGBT, conventional RC-IGBT, TPRC-IGBT, and the DARC-IGBT. The inset picture shows the inductive load turn off circuit, the bus voltage V_{bus} = 350 V, The gate resistance R_g = 10 Ω, the load resistance R_C = 3.5 Ω, and the stray inductance L_S = 200 nH.

RC-IGBT and the TPRC-IGBT have superior reverse conduction property with V_R less than 1.0 V at the current density of 100A/cm^2. The DARC-IGBT has the highest V_R more than 3.0 V due to the shield effect of the additional anode. For the proposed LDT-RC-IGBT, the V_R can be further optimized to 1.39 V by the increase of the doping of the EPR.

Fig. 8 shows the reverse recovery characteristics of the RC-IGBTs. The DARC-IGBT has faster switching speed and less reverse recovery charge Q_{rr} of 10.5 μc/cm^2. The TPRC-IGBT and the conventional have larger Q_{rr} of 52.7 μc/cm^2 and 47.4 μc/cm^2 due to the more nonequilibrium carriers are stored at the reverse conduction. For the proposed, the Q_{rr} can be decreased by the decrease of the doping of the EPR.

D. TURN-OFF CHARACTERISTICS

Fig. 9 shows the dynamic characteristics of the RC-IGBTs, the devices are turned off under the same inductive load

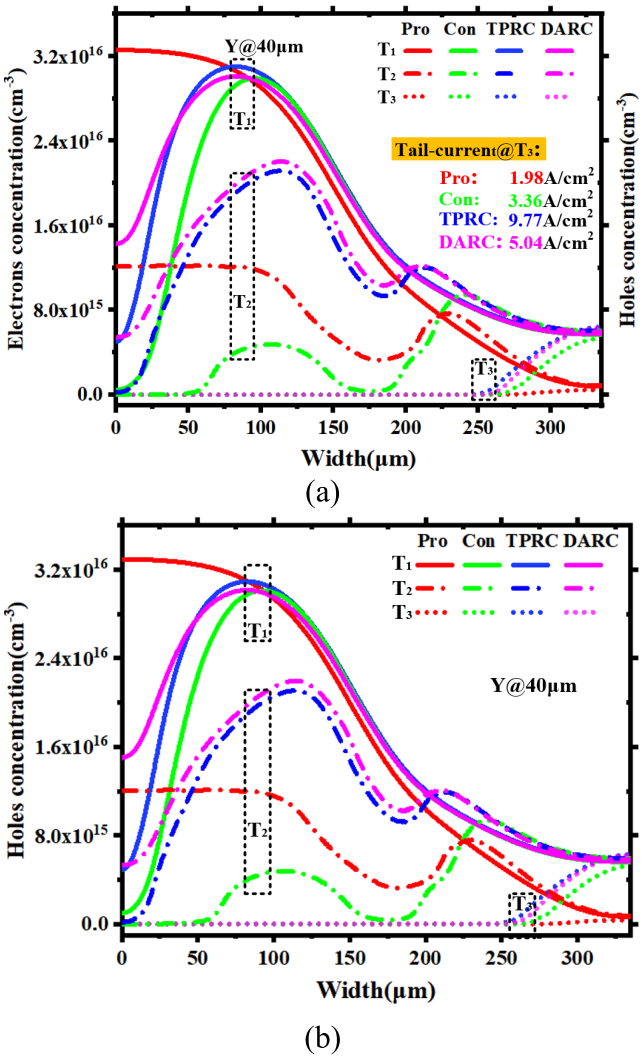

FIGURE 10. The carriers concentration in Active cell region at *X*-direction (*Y*=40 μm) during the turn-off process from T_1 toT_3 for the proposed, conventional RC-IGBT, TPRC-IGBT, and DARC-IGBT, the T_1, T_2 and T_3 are given in Fig. 9.(a) electrons concentration distribution (b) holes concentration distribution.

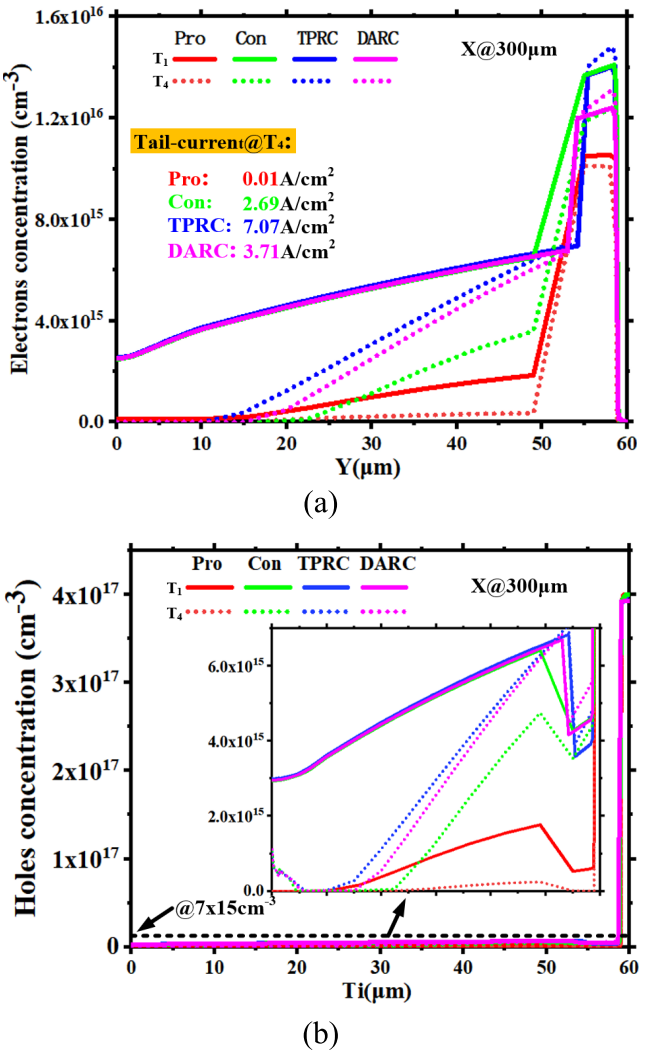

FIGURE 11. The carriers concentration in Terminal region at *Y*-direction (*X*=300μm) during the turn-off process from T_1 to T_4 for the proposed, conventional RC-IGBT, TPRC-IGBT, and DARC-IGBT, theT_1 and T_4 are given in Fig. 9.(a) electrons concentration distribution (b) holes concentration distribution.

circuit. The turn-off time T_{off} is calculated from 90% I_c to 10% I_c and the tail-current is defined below 10% I_c. For the conventional RC-IGBT, it has the shortest T_{off} with 96 ns due to the extraction of the N-Collector. For the proposed, the T_{off} is 131 ns which is decreased by 8.3% and 26% compared with the DARC-IGBT(143 ns) and TPRC-IGBT(177 ns), respectively. Additionally, the tail-current of the conventional RC-IGBT, TPRC-IGBT and DARC-IGBT are much longer than the proposed due to the injection of the holes from the P-Collector during the turn off process.

Fig. 10(a) and Fig. 10(b) shows the electrons and holes concentration of the active cell region in X-direction (Y = 40 μm) respectively for the RC-IGBTs from $T_1$to T_3 period in Fig. 9. Where the turn off current begins to decrease from T_1. It can be seen that both of the electrons and holes concentration in the N-drift of the conventional RC-IGBT and proposed are much lower than that of the TPRC-IGBT and DARC-IGBT during the turn off process at T_2, and the tail-current of the proposed is the lowest at T_3.

Fig. 11(a) and Fig. 11(b) shows the electrons and holes concentration of the terminal region in Y-direction (X = 300 μm) respectively for the RC-IGBTs from T_1 to T_4. It can be seen that the turn off current at T_1 and the tail-current at T_4 of the proposed are the lowest due to the carrier extraction of the N-stopper/N-collector in the termination region.

Fig. 12 shows the trade-off relationships between V_{on} and E_{off} of the RC-IGBTs. the proposed LDT-RC-IGBT realizes 35.2%, 45.2% and 46.3% reduction on E_{off} at the same V_{on} of 1.27 V compared with the conventional RC-IGBT, TPRC-IGBT and DARC-IGBT, respectively. In addition, the V_{on} of the proposed LDT-RC-IGBT is 10%, and 15.8% lower than the conventional RC-IGBT and the DARC-IGBT,

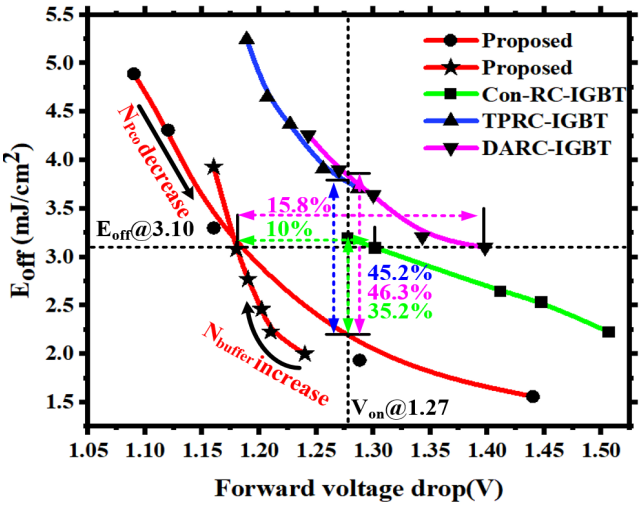

FIGURE 12. Trade-off performance between E_{off} and V_{on} of the proposed, conventional RC-IGBT, TPRC-IGBT, and the DARC-IGBT at current density of 100 A/cm^2.

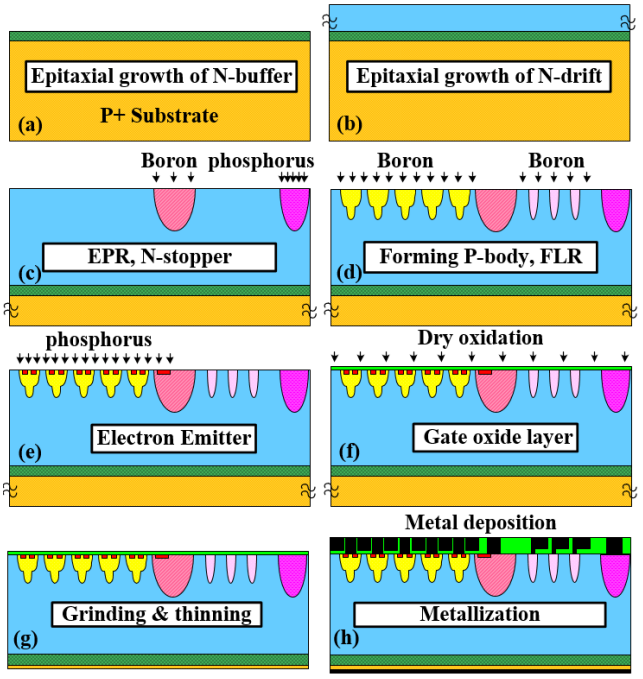

FIGURE 13. The key process for the LDT-RC-IGBT (a) P+ substrate with N-buffer (b) Epitaxy N-drift (c) Implantation for the EPR and N-stopper of the FWD (d) Implantation for the P-body and the FLR (e) Implantation for the cathode N+ (f) thermal growth of gate oxide (g) grinding the P-sbustrate (h) metallization for the cathode, anode and gate electrode.

respectively at the same E_{off} of 3.10 mJ/cm^2, which realizes a superior trade-off property.

E. KEY PROCESSES

Fig. 13 depicts the key process steps of the fabrication for the LDT-RC-IGBT. The device is based on the P+ substrate with epitaxial N-buffer in Fig. 13(a). The N-drift is grew by epitaxy in Fig.13(b). The EPR and the N-stopper/N-Collector of the FWD are realized by the Boron and phosphorus implantation in Fig. 13(c).

The P-body and the FLR are realized by the Boron implantation in Fig. 13(d). The cathode N+ is realized by phosphorus implantation in Fig. 13(e). The gate oxide SiO_2 is formed by oxidation and etching in Fig. 13(f). The P+ substrate is ground to form P-Collector in Fig. 13(g). Finally the cathode, anode and gate electrode are metallized and etched in Fig. 13(h), the fabrication process is compatible with the conventional IGBTs. Additionally the N-collector and the P-collector are shorted together, which can be realized by the external bonding or the TSV (Through Silicon Via).

IV. CONCLUSION

The proposed LDT-RC-IGBT not only eliminates the snapback but also reduces V_{on} at the forward conduction, thus a better trade-off between BV and V_{on} is achieved. The FWD is laterally integrated by the EPR and N-stopper in the termination, but the reverse conduction V_R needs to be further optimized. However, a much better trade-off between V_{on} and E_{off} is realized compared with the conventional RC-IGBT, TPRC-IGBT and DARC-IGBT.

REFERENCES

[1] K. Komatsu, M. Yatsu, S. Miyashita, S. Okita, H. Nakazawa, S. Igarashi, Y. Takahashi, Y. Okuma, Y. Seki, and T. Fujihira, "New IGBT modules for advanced neutral-point-clamped 3-level power converters," in *Proc. Int. Power Electron. Conf.-ECCE ASIA*, Sapporo, Japan, Jun. 2010, pp. 523–527, doi: 10.1109/IPEC.2010.5543275.

[2] H. Hoffmann and B. Piepenbreier, "High voltage IGBTs and medium frequency transformer in DC-DC converters for railway applications," in *Proc. SPEEDAM*, Pisa, Italy, Jun. 2010, pp. 744–749, doi: 10.1109/SPEEDAM.2010.5542109.

[3] Z. Y. Sun, F. Yang, Y. Sun, and B. Cui, "Study on heat dissipation performance of IGBT module in wind power converter," in *Proc. IEEE Int. Conf. Appl. Supercond. Electromagn. Devices*, Beijing, China, Oct. 2013, pp. 233–236, doi: 10.1109/ASEMD.2013.6780751.

[4] R. Gejo, T. Ogura, S. Misu, Y. Maeda, Y. Matsuoka, N. Yasuhara, and K. Nakamura, "High switching speed trench diode for 1200V RC-IGBT based on the concept of Schottky Controlled injection (SC)," in *Proc. 28th Int. Symp. Power Semiconductor Devices ICs (ISPSD)*, Prague, Czech Republic, Jun. 2016, pp. 155–158, doi: 10.1109/ISPSD.2016.7520801.

[5] H. Jiang, B. Zhang, W. Chen, C. Liu, Z. Rao, and B. Dong, "A snapback suppressed reverse-conducting IGBT with a floating p-region in trench collector," in *Proc. Asia–Pacific Power Energy Eng. Conf.*, Shanghai, China, Mar. 2012, pp. 1–4, doi: 10.1109/APPEEC.2012.6307221.

[6] T. Yoshida, T. Takahashi, K. Suzuki, and M. Tarutani, "The second-generation 600V RC-IGBT with optimized FWD," in *Proc. 28th Int. Symp. Power Semiconductor Devices ICs (ISPSD)*, Prague, Czech Republic, Jun. 2016, pp. 159–162, doi: 10.1109/ISPSD.2016.7520802.

[7] L. Cui, B. J. Zhang, P. F. Wu, L. Ma, R. L. Zhang, and Z. B. Zhao, "A snapback-free RC-IGBT with Si_3N_4 trench and P-type pillar," in *Proc. IEEE Int. Conf. Electron Devices Solid-State Circuits (EDSSC)*, Xi'an, China, Jun. 2019, pp. 1–3, doi: 10.1109/EDSSC.2019.8754350.

[8] M. Antoniou, F. Udrea, F. Bauer, and I. Nistor, "A new way to alleviate the RC IGBT snapback phenomenon: The Super Junction solution," in *Proc. 22nd Int. Symp. Power Semiconductor Devices IC's (ISPSD)*, Hiroshima, Japan, Jun. 2010, pp. 153–156.

[9] J. Oh, D. H. Chun, R. Oh, and H. S. Kim, "A snap-back suppressed shorted-anode lateral trench insulated gate bipolar transistor (LTIGBT) with insulated trench collector," in *Proc. IEEE Int. Symp. Ind. Electron.*, Jun. 2011, pp. 1367–1370.

[10] W. Chen, Z. Li, M. Ren, J. Zhang, B. Zhang, Y. Liu, Q. Hua, K. Mao, and Z. Li, "A high reliable reverse-conducting IGBT with a floating P-plug," in *Proc. 25th Int. Symp. Power Semiconductor Devices IC's (ISPSD)*, Kanazawa, Japan, May 2013, pp. 265–268, doi: 10.1109/ISPSD.2013.6694437.

[11] B. Yi, Z. Lin, and X. Chen, "Snapback-free reverse-conducting IGBT with low turnoff loss," *Electron. Lett.*, vol. 50, no. 9, pp. 703–705, Apr. 2014, doi: 10.1049/el.2014.0169.
[12] L. Zhu and X. Chen, "An investigation of a novel snapback-free reverse-conducting IGBT and with dual gates," *IEEE Trans. Electron Devices*, vol. 59, no. 11, pp. 3048–3053, Nov. 2012, doi: 10.1109/TED.2012.2215039.
[13] H. Jiang, B. Zhang, W. Chen, C. Liu, Z. Rao, and B. Dong, "A snapback suppressed reverse-conducting IGBT with a floating p-region in trench collector," *IEEE Electron Device Lett.*, vol. 33, no. 3, pp. 417–419, Mar. 2012, doi: 10.1109/LED.2011.2180357.
[14] W. Chen, B. Zhang, Z. Li, M. Ren, and Z. Li, "A short-contacted double anodes IGBT," in *Proc. IEEE 11th Int. Conf. Solid-State Integr. Circuit Technol.*, Xi'an, China, Oct./Nov. 2012, pp. 1–3, doi: 10.1109/ICSICT.2012.6467705.
[15] L. Storasta, A. Kopta, and M. Rahimo, "A comparison of charge dynamics in the reverse-conducting RC IGBT and Bi-mode Insulated Gate Transistor BiGT," in *Proc. 22nd Int. Symp. Power Semiconductor Devices IC's (ISPSD)*, Hiroshima, Japan, Jun. 2010, pp. 391–394.
[16] J. Wei, X. Luo, L. Huang, and B. Zhang, "Simulation study of a novel snapback-free and low turn-off loss reverse-conducting IGBT with controllable trench gate," *IEEE Electron Device Lett.*, vol. 39, no. 2, pp. 252–255, Feb. 2018, doi: 10.1109/LED.2017.2780081.
[17] E. Griebl, L. Lorenz, and M. Purschel, "LightMOS a new power semiconductor concept dedicated for lamp ballast application," in *Proc. 38th IAS Annu. Meeting Conf. Rec. Ind. Appl. Conf.*, vol. 2. Salt Lake City, UT, USA, Oct. 2003, pp. 768–772.

WEIZHONG CHEN received the Ph.D. degree in microelectronics from the University of Electronic Science and Technology of China (UESTC), Chengdu, China, in 2014. He was a Visiting Scholar with the Fraunhofer Institute for Integrated Systems and Device Technology IISB, Erlangen, Germany, in 2018. He holds a postdoctoral position at the Institute of Microelectronics of Chinese Academy of Sciences, Beijing, China, in 2019, and also an Associate Professor of the College of Electronics Engineering, Chongqing University of Posts and Telecommunications. He has authored or coauthored over 30 articles. He holds over 20 Chinese patents. His research interests include power devices and integrated power systems.

YAO HUANG received the bachelor's degree in microelectronics from the College of Electronics Engineering, Chongqing University of Posts and Telecommunications. He is currently pursuing the master's degree in microelectronics.

SHUN LI received the bachelor's degree in microelectronics from the College of Electronics Engineering, Chongqing University of Posts and Telecommunications. He is currently pursuing the master's degree in microelectronics.

YI HUANG received the Ph.D. degree in microelectronics from the Nanjing University of China, Nanjing, China, in 2012. He is currently an Associate Professor of the College of Electronics Engineering, Chongqing University of Posts and Telecommunications. He has authored or coauthored over 20 articles. He holds over 20 Chinese patents.

ZHENGSHENG HAN is currently a Professor of the Institute of Microelectronics of Chinese Academy of Sciences, Beijing, China, and the University of Chinese Academy of Sciences, Beijing. He has authored or coauthored over 100 articles. He holds over 40 Chinese patents. His research interests include power devices and power systems.